frontiers in Materials

ORIGINAL RESEARCH
published: 04 March 2022
doi: 10.3389/fmats.2022.852731

pH-Responsive Allicin-Based Coatings With Antibacterial and Antifouling Effects in Marine Environments

Xiangping Hao[1,2†], *Weilu Yan*[1,2†], *Ziqing Sun*[1], *Jingzhi Yang*[1,2], *Yun Bai*[1,2], *Hongchang Qian*[1,2], *Thee Chowwanonthapunya*[3,2*] *and Dawei Zhang*[1,2*]

[1]National Materials Corrosion and Protection Data Center, Institute for Advanced Materials and Technology, University of Science and Technology Beijing, Beijing, China, [2]BRI Southeast Asia Network for Corrosion and Protection (MOE), Shunde Graduate School of University of Science and Technology Beijing, Foshan, China, [3]Faculty of International Maritime Studies, Kasetsart University, Chonburi, Thailand

In this work, we report the design of pH-controlled releasing behaviors of polydopamine/tannic acid-allicin@chitosan (PDA/TA-ALL@CS) multilayer coatings to realize antibacterial and antifouling effects. The pH-responsive ALL@CS capsules were prepared using the microemulsion method with about 262–452 nm diameter. The bacteriostasis of ALL@CS microcapsules against *E. coli*, *S. aureus*, and *P. aeruginosa* all exceeded 94% as evaluated using the colony counting method. Because of the protonation in acid environments and deprotonation in alkaline environments for the amino groups of CS, ALL as biocides can be released from the nanocapsules and exert outstanding antibacterial properties. Confirmed by the plate colony counts, the ALL@CS capsules possessed an outstanding antibacterial effect for *E. coli* in acid solutions but were less effective in alkaline solutions. The PDA/TA-ALL@CS-7 coatings showed durable pH-responsive antibacterial activities with an efficiency of ~87% after immersion in pH 8 solutions for seven days. The PDA/TA-ALL@CS coating with controlled release performance and antibacterial properties may provide a new solution for developing antifouling coating applications in the marine environment.

Keywords: antibacterial, antifouling, pH-responsive, nanocapsules, marine environment

OPEN ACCESS

Edited by:
Xiaoqiang Fan,
Southwest Jiaotong University, China

Reviewed by:
Helena P. Felgueiras,
University of Minho, Portugal
Wei Wang,
Ocean University of China, China

***Correspondence:**
Dawei Zhang
dzhang@ustb.edu.cn
Thee Chowwanonthapunya
thee.c@ku.th

†These authors have contributed equally to this work

Specialty section:
This article was submitted to Environmental Degradation of Materials, a section of the journal Frontiers in Materials

Received: *11 January 2022*
Accepted: *11 February 2022*
Published: *04 March 2022*

Citation:
Hao X, Yan W, Sun Z, Yang J, Bai Y, Qian H, Chowwanonthapunya T and Zhang D (2022) pH-Responsive Allicin-Based Coatings With Antibacterial and Antifouling Effects in Marine Environments. Front. Mater. 9:852731. doi: 10.3389/fmats.2022.852731

INTRODUCTION

Biofouling issue in the marine environment brings a series of problems such as decreasing the speed of vehicles, increasing economic losses, and triggering the invasion of exotic species (Lejars et al., 2012). The conventional method comprises painted antifouling coatings containing biocides to restrain the biofouling process of the substrate underwater (Yebra et al., 2004; Banerjee et al., 2011; Bagley et al., 2015; Hao et al., 2016; Jia et al., 2017; Bloecher et al., 2021; Liu et al., 2021). The antifouling property of the coatings is realized through releasing of the antifoulant from the coating, so the releasing rate of the antifoulant is an important issue when designing coatings. Generally, the speed of vehicles has a huge impact on the releasing rate of the antifoulant, and the releasing rate is virtually much higher at high speed (Hao et al., 2020). At the anchor state, the coatings often cannot protect the substrates completely because the microorganism colonization occurs easily, but antifoulant release is more difficult. Hence, exploring antifouling coatings that release

antifoulant as required, especially at low-speed and at anchor states, is a critical guide for the future. Because the secretions such as acetic acid and lactic acid produced by bacterial metabolisms can decrease the pH of the microenvironment to acidic (Qian et al., 2007a; Traba and Liang, 2015; Hao et al., 2019; Saadouli et al., 2021), pH-responsive antifouling coatings have attracted increasing attention and developed rapidly in recent years (Hao et al., 2019; Hao et al., 2020; Huang et al., 2020; Xu et al., 2020).

Chitosan (CS) as a cationic natural polysaccharide not only possesses antibacterial properties but also is a proper candidate for preparing pH-responsive nanocapsules as a shell material because of the protonation and deprotonation of the amino groups (Chen et al., 2021; Hosseini et al., 2022; Tian et al., 2022). Wang et al. and Andrew et al. provided that CS can help to control drug-releasing behaviors by adjusting diffusion, swelling, and stimulus response (Arifin et al., 2006; Lin and Metters, 2006). Cheng et al. designed biodegradable pH-responsive hollow mesoporous silica nanoparticles for the delivery of pheophorbide and doxorubicin. These carriers demonstrated pH-sensitive drug delivery because of the GM/CS capping layer (Yan et al., 2020). Arash et al. prepared a smart drug delivery system using CS nanocapsule-mounted cellulose nanofibrils, and the optimal release of metronidazole molecules was pH 5.8 (Yunessnia lehi et al., 2019). In addition to the wide application in drug delivery and biomedical fields, CS as a representative has also been used to design pH-responsive antifouling systems to acquire smart and controlled releasing of antifoulants. When the bacteria colonize and reproduce near the motionless substrates, the pH of microenvironments will change from alkaline to acidic, and trigger protonation of the amino groups on the side chain of CS, leading to the swelling of the nanocapsules and accelerated releasing of the biocides. Chen et al. had used CS as a capped layer to encapsulate capsaicin, and the amount of released capsaicin was five times higher in a pH 4 environment than that in pH 8.5 (Wang et al., 2018). The abovementioned studies show that precise releasing of antifoulants in the marine environment can be realized by virtue of the pH-responsive character of CS, thus preventing the substrates from biofouling at anchor states and extending the longevity of antifouling coatings.

With the development of low copper and copper-free antifoulants, synthetic and natural biocides have been extensively studied as alternatives to prepare antifouling coating with excellent bactericidal performance (Qian et al., 2007b; Huang et al., 2019; Qian et al., 2019; Yang et al., 2021). Allicin (ALL), as one of the active components of freshly crushed garlic homogenates, has many advantages like broad-spectrum antibacterial effect at low concentrations, anticancer activity, and being less likely to develop bacterial drug resistance (Ankri and Mirelman, 1999; Bhatwalkar et al., 2021; Greef et al., 2021). In addition, Rajaneesh et al. demonstrated that garlic and its compounds have a positive effect on human beings by inhibiting reactive oxygen species, radical scavenging, and preventing DNA damage (Cao et al., 2014; Zhang et al., 2020; Bhatwalkar et al., 2021). Moreover, Breyer showed that garlic compound (ALL) can eliminate mortality on rainbow trout infected with *Aeromonas hydrophila* (Breyer, 2013). These kinds of literature prove that the ALL as an antifoulant is not only harmless to human beings but also has no side effect on marine vertebrates. However, the low stability and solubility of ALL restrict its applications. The disulfide bond, which is the main resource of the antibacterial properties in ALL, is particularly prone to rupture under alkaline conditions (Wills, 1956). One popular approach to solve this problem is to encapsulate allicin with proper encapsulation (Lawson and Hughes, 1992; Janská et al., 2021). For example, Malgorzata et al. designed oil-core nanocapsules based on a derivative of hyaluronic acid to protect garlic oil active components, resulting in preventing sulfur oxidation and maintaining antibacterial activities (Janik-Hazuka et al., 2021). Based on the previous discussion, it is believed that encapsulation of ALL in pH-responsive microcapsules could effectively improve the stability of ALL and achieve the purpose of a pH-controlled releasing process of the antifoulant.

Herein, the pH-responsive ALL@CS nanocapsules which were prepared by microemulsions were mixed with tannic acid (TA) as an anionic polyelectrolyte, followed by alternating deposition with polydopamine (PDA) which has an outstanding film-forming ability to acquire the pH-responsive PDA/TA-ALL@CS-n antifouling coatings. The ALL@CS nanocapsules with different diameters were obtained by adjusting the weight ratio of ALL and CS, and the PDA/TA-ALL@CS-n were prepared by adjusting the doping ratio of ALL@CS nanocapsules in TA solutions. The composite and size of the nanocapsules were evaluated using Fourier transform infrared spectroscopy (FTIR) and dynamic light scattering (DLS). The pH-responsive antibacterial properties of the nanocapsules were detected using DLS and the plate colony method. The composition, morphology, and thickness of the coatings were characterized using FTIR and scanning electron microscope (SEM). The antifouling and antibacterial performance of the PDA/TA-ALL@CS-n coatings were evaluated using the colony counting method and live/dead fluorescence. The ALL releasing behavior in different pH environments was measured using an ultraviolet–visible spectrophotometer (UV-Vis), and the pH-responsive antibacterial properties of the coatings were characterized using the colony counting method.

EXPERIMENTAL SECTION

Materials

CS with a low viscosity <200 mPa S and Tris (hydroxymethyl) aminomethane were provided by Aladdin Chemistry Co. Ltd. (China). ALL with a purity >95%, lecithin with a purity >98%, and dopamine hydrochloride were purchased from Shanghai Macklin Biochemical Co. Ltd. (China). TA was purchased from Sigma-Aldrich (United States). Different pH phosphate-buffered saline (PBS) solutions were stored after sterilization. Live/dead® BacLight TM Bacterial Viability Kit (L13152) was obtained from Thermo Fisher Scientific (America). The *E. coli* (ATCC 8739), *S. aureus* (ATCC 6538), and *P. aeruginosa* (MCCC 1A00099) were purchased from the Institute of Microbiology, Chinese Academy of Sciences, Beijing, China.

Preparation of ALL@CS Nanocapsules

The ALL@CS nanocapsules were synthesized using the microemulsion method (Wang et al., 2018). Different volumes of ALL (60, 35, and 10 μL) were added into the lecithin-containing ethyl alcohol solution. 10 mg of CS was mixed with an aqueous solution with 1% v/v acetic acid. These two solutions were mixed and stirred at room temperature for 2 h, followed by dialysis, to eliminate free ALL and freeze-drying.

Preparation of PDA/TA-ALL@CS-n Coatings

The 316L stainless steel substrates were abraded to 1200 grit with silicon carbide papers and cleaned with acetone, ethanol, and distilled water in ultrasonic baths. After drying with N_2, the coupons were immersed in dopamine hydrochloride (2 mg/ml) with Tris buffer (100 mM, pH 8.5) for 15 min at room temperature in a dark place, and then washed with distilled water smoothly, followed by immersion in different TA-ALL@CS solutions for another 15 min. The volume ratio of TA solution (2 mg/ml) and ALL@CS suspension (1 mg/ml) was 6:4, 7:3, and 8:2. The substrates were alternately dopped in these two solutions according to the abovementioned process about 20 times and dried with N_2.

Antimicrobial Properties of ALL@CS Nanocapsules

The colony counting method was applied to evaluate the antimicrobial ability of the ALL@CS nanocapsules. The initial concentration of each bacterium was about ~10^8 CFU/ml. Every 1 ml of *E. coli* or *S. aureus* suspensions was transformed into 50 ml Luria broth (LB) and incubated at 37°C for 18 h, and 1 ml *P. aeruginosa* suspensions were transformed into 2216 E medium culture and incubated at 30°C for 18 h. Afterward, 200 μL cultivated bacterial suspension was inoculated into 10 ml LB or 2216 E culture medium containing 1 mg/ml CS, ALL, or ALL@CS nanocapsules, and incubated for another 18 h at 37°C or 30°C. 20 μL suspension of each bacterial tube was diluted with physiological saline and spread on a solid medium plate, incubating overnight at corresponding temperature conditions.

pH-Responsive Performance and Antibacterial Properties of ALL@CS Nanocapsules

The ALL releasing behavior in different pH environments was evaluated initially. The dialysis bags with ALL@CS nanocapsule suspension were dialyzed at different pH PBS (pH 5, 6, 7, and 8) solutions for 4 h. The size of the ALL@CS nanocapsules was detected using DLS.

The pH-responsive properties of such nanocapsules were further measured using the colony plate method. The *E. coli* suspension was inoculated into 10 ml PBS solutions (pH 5, 6, 7, and 8) and LB with a 1:1 volume ratio containing ALL@CS nanocapsules, respectively. After incubation for 4 h, 20 μL diluted bacterial suspension was spread on the top of the solid medium and cultivated at 37°C for 18 h.

Antifouling and Antibacterial Properties of PDA/TA-ALL@CS-n Coatings

The colony counting method and live/dead fluorescence analysis were used to evaluate the antimicrobial ability of the PDA/TA-ALL@CS-n coatings. The initial concentration of each bacterium was about ~10^8 CFU/ml. Every 1 ml of *E. coli* or *S. aureus* suspensions was transformed into 50 ml LB and incubated at 37°C for 18 h, and 1 ml *P. aeruginosa* suspension was transformed into 2216E medium culture and incubated at 30°C for 18 h. Thereafter, 200 μL cultivated bacterial suspension was inoculated in a 10-ml sterile tube with different PDA/TA-ALL@CS-n-coated substrates. After incubation for 18 h, 20 μL diluted bacterial suspensions were spread on the top of the solid medium at 37°C or 30°C for 18 h.

The antibacterial and antifouling performances of the PDA/TA-ALL@CS-n coatings were detected using a confocal laser scanning microscope using a Live/dead® BacLight TM Bacterial Viability Kit. Each coated coupon was immersed in different bacterial suspensions for 18 h, and surfaces of the coupons were dyed at a 6-well plate for 20 min at dark places.

pH-Responsive Properties of PDA/TA-ALL@CS-n Coatings

The coated substrates were immersed in 0.1 M different PBS environments with pH values of 5–8 in a static environment. The concentrations of released ALL in different PBS solutions were measured spectroscopically at around 210 nm by UV-Vis after immersion for one, three, five, and seven days (Hathout et al., 2018). The coated coupons were collected, washed with diluted water, and dried with N_2 to detect the antibacterial properties.

The collected coupons were sterilized and taken into the sterile tube containing 200 μL *S. aureus* or *P. aeruginosa* in 10 ml LB or 2216 E culture medium. The suspensions were shaken at 120 rpm and incubated at 37°C or 30°C for 18 h, and each 20 μL diluted bacterial suspension was taken for colony counting by spreading on the solid medium plate and incubating overnight at different temperature conditions.

Characterization

The size and zeta potential of the ALL@CS nanocapsules were detected using Zetasizer Nano ZS90 (Malvern Instrument, Britain). The FTIR VERTEX70 was manufactured by Burker (Germany). The thickness and the morphology of the PDA/TA-ALL@CS-n coatings were demonstrated using SEM (Jeol JSM-F100, Japan). The UV-Vis used was manufactured by Thermo Biomates 3S (Thermo, America). The CLSM (Zeiss Observer Z1, Germany) was applied to determine the fluorescent assay.

RESULTS AND DISCUSSION

Characterization of the Prepared ALL@CS Nanocapsules

FTIR spectra of the CS, ALL, and the product we prepared are evaluated and demonstrated in **Figure 1**. On the ALL spectrum,

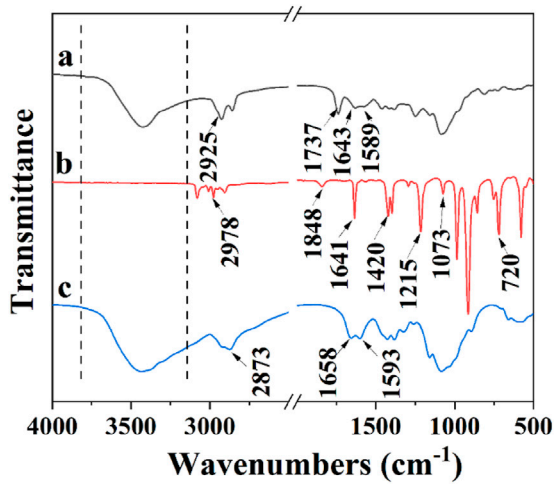

FIGURE 1 | FTIR spectra of ALL@CS **(A)**, ALL **(B)**, and CS **(C)**.

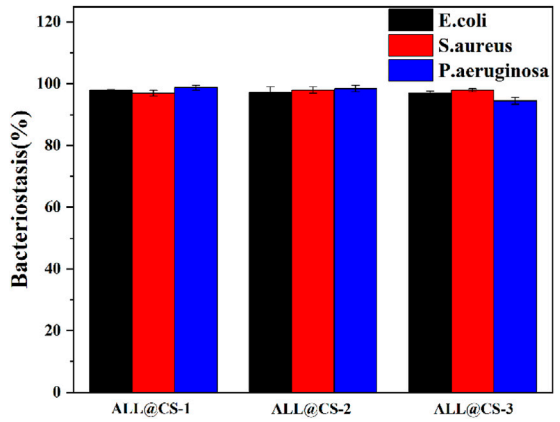

FIGURE 2 | Bacteriostasis of different ALL@CS nanocapsules against *E. coli*, *S. aureus*, and *P. aeruginosa*.

TABLE 1 | Mean hydrodynamic diameter, PDI, and zeta potential of nanocapsules made using different proportions of CS and ALL.

No	CS (mg)	ALL (μL)	Size (nm)	PDI	Zeta potential (mV)
1	10	60	261.7 ± 3.9	0.54 ± 0.07	7.7 ± 1.1
2	10	35	333.8 ± 3.5	0.32 ± 0.07	32.8 ± 1.6
3	10	10	452.3 ± 1.5	0.33 ± 0.01	40.6 ± 0.2
4	10	/	/	/	41.7 ± 0.4
5	/	60	/	/	−25.9 ± 0.7

the peaks at 2978 cm^{-1} and 1420 cm^{-1} belong to C-H stretching (Zhou et al., 2021). 1641 cm^{-1} and 1073 cm^{-1} peaks are associated with the C=C stretching vibration and S=O stretching vibration, respectively. The peaks at 1215 cm^{-1} and 720 cm^{-1} are attributed to S-S single bond (Kumar et al., 2021; Zhou et al., 2021). As for the spectrum of products, it is similar to the CS spectrum. The broad peak at 3300–3200 cm^{-1} can be seen in these two spectra which are contributed with the O-N and N-H stretching vibration (Lawrie et al., 2007). 2873 cm^{-1} peak on CS spectrum and 2925 cm^{-1} on product spectrum are associated with the C-H stretching vibration. The peaks located at 1658 cm^{-1} and 1593 cm^{-1} which belong to the N-H bending vibration of the amino group appear on the spectrum a at 1643 cm^{-1} and 1589 cm^{-1} (Wang et al., 2018). In addition, the new peak appears at 1737 cm^{-1} on the spectrum a because of the H-bond between CS and ALL (Gu et al., 2018). The 1848 cm^{-1} on the ALL curve is disappeared in spectrum a, indicating the inclusion interaction between ALL and CS attenuated the absorption of the guest molecular moiety (Zhou et al., 2021).

Table 1 summarizes the mean diameter, polydispersity index (PDI), and zeta potential of the ALL@CS nanocapsules synthesized at different weight ratios with CS and ALL. The zeta potential is positive for CS but is negative for pure ALL. The nanocapsules are all positively charged like CS, suggesting that the negative surface charge of free ALL is completely covered by cationic CS. This result agrees well with the FTIR result. Moreover, the ratio of CS and ALL impacts the zeta potential and diameter of the ALL@CS nanocapsules. With the decrease of the ratio, the size of the nanocapsules increases from 261.7 ± 3.9 nm to 452.3 ± 1.5 nm and the zeta potential increases from 7.7 ± 1.1 mV to 40.6 ± 0.2 mV. According to the DLVO theory, the stability of the system becomes lower as the size of the ALL@CS nanocapsules decreases because the balance between the Van der Waals force and the electrostatic repulsive force is broken (Hao et al., 2019). It means the ALL@CS-1 nanocapsule systems are not stable, and the zeta potential data also support this conclusion.

Antibacterial Properties and pH-Responsive Mechanism of ALL@CS Nanocapsules

E. coli and *S. aureus* were selected as representative Gram-negative bacterium and Gram-positive bacterium, and *P. aeruginosa* was selected as the marine bacteria representative strain. The antibacterial properties of three kinds of ALL@CS nanocapsules were evaluated using the colony counting method to choose the optimal preparation parameter. In **Figure 2**, all of these nanocapsules exhibit outstanding antibacterial effects, with the bacteriostasis rates ranging from 94.5 to 98.7%. The antibacterial properties of All@CS-3 nanocapsules are relatively poor of the three different diameter nanocapsules, and the bacteriostasis rates of *E. coli*, *S. aureus*, and *P. aeruginosa* are about 97.0, 98.0, and 94.5%, respectively. ALL@CS-1 and All@CS-2 nanocapsules show similar antibacterial properties, which surpass 97.03% against these three different bacterial strains. Considering the stability of the nanocapsules shown in **Table 1** and the ALL dosage, ALL@CS-2 nanocapsules were selected in the following study.

The antibacterial properties of pure CS, ALL, and ALL@CS nanocapsules were further evaluated using the colony counting method. Generally, CS and ALL have excellent antibacterial properties, and the antibacterial effect improves after synthesis

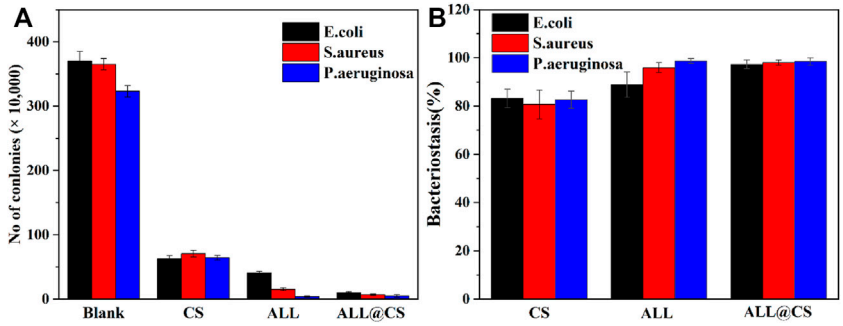

FIGURE 3 | Number of *E. coli*, *S. aureus*, and *P. aeruginosa* colonies in LB and 2216E medium for 18 h with pure CS, ALL, and ALL@CS nanocapsules **(A)**. The bacteriostasis of these three different bacteria strains corresponding to each counting result **(B)**.

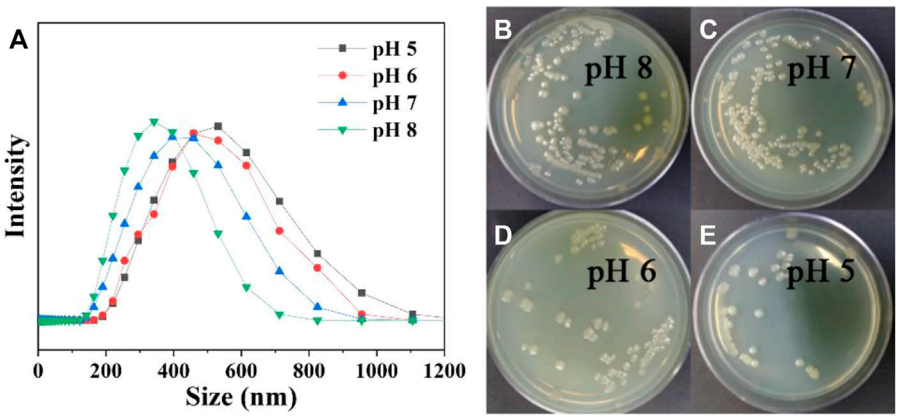

FIGURE 4 | Size of ALL@CS nanocapsules in different pH PBS solutions **(A)**. The plate colony images of ALL@CS incubating with *E. coli* for about 4 h **(B–E)**.

of ALL@CS as shown in **Figure 3**. In **Figure 3A**, after incubation for 18 h, the colonies of *E. coli* on the solid medium are about 370 CFU for the control group, and there are about 63, 41, and 10 CFU after incubation with the pure CS, ALL, and ALL@CS nanocapsules. According to **Figure 3B**, the bacteriostasis rate of ALL@CS against *E. coli* is 97.3%, which is increased by ~14.3 and ~8.4% compared with that of pure CS and ALL. The bacteriostasis rates of pure CS, ALL, and ALL@CS nanocapsules against *S. aureus* are 80.6, 95.9, and 98.0%, respectively. Regarding the antibacterial effects on *P. aeruginosa*, there are approximately 323 CFU for the control group and 5 CFU of the group with ALL@CS; that is, the bacteriostasis rate of ALL@CS is ~98.5%. The results revealed that the antibacterial properties of the ALL after encapsulating CS were almost unaffected or even slightly improved.

The pH-responsive properties of the ALL@CS nanocapsules were evaluated using DLS and the colony plate method. In **Figure 4A**, with the pH of the PBS environment decreasing from 8 to 5, the size of the ALL@CS increases from about 342.0 to 531.2 nm because of the protonation of the amino group CS. Under acidic conditions (i.e., pH 5 and 6), the ALL@CS nanocapsules exhibit swelling behaviors because the internal electrostatic repulsion of the system increased resulting from the NH_2 transformation to NH_3^+ (Lee and Mooney, 2012; Hao et al., 2019). However, the nanocapsules can remain at a smaller diameter which is about 396.1 and 342.0 nm in a neutral and alkaline environment, respectively. Meanwhile, the antibacterial performance against *E. coli* under different pH environments is different. **Figures 4B–E** demonstrate that after being treated with pH 8 and 7 solutions, the number of colonies is more than that with the pH 6 and 5 counterparts, and the colony count is minimal on the solid medium after incubation in pH 5 PBS environments, indicating that the ALL@CS nanocapsules have better antibacterial properties in acidic environments. Combined with the DLS results, the ALL@CS nanocapsules are swollen under an acidic environment, leading to the increased amount of released ALL and thus the stronger antibacterial effect. On the contrary, under the neutral and alkaline environment, the nanocapsules present a smaller diameter which restricts the releasing of ALL and leads to an inhibited antibacterial property. Hence, the ALL can be kept in the nanocapsules under alkaline conditions such as marine environments, and kill bacteria when the pH value drops due to bacteria reproduction under the anchoring state.

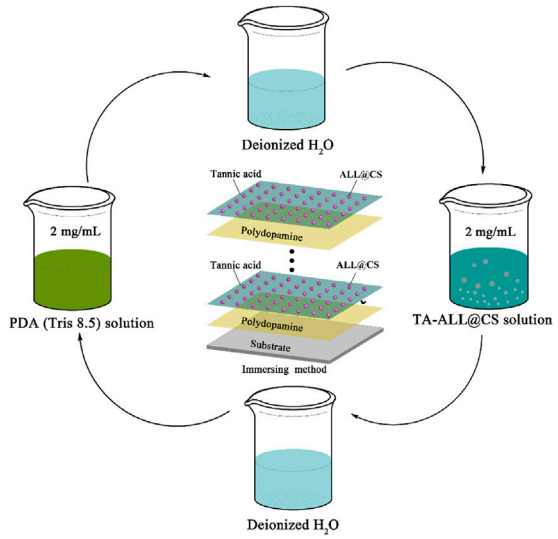

FIGURE 5 | Schematic diagram of the preparation procedure of PDA/TA-ALL@CS coatings.

Characterization of the Prepared PDA/TA-ALL@CS Coatings

The PDA/TA@ALL@CS coatings were fabricated by a layer-by-layer technique as shown in **Figure 5**, and the FTIR spectra of TA, PDA, TA-ALL@CS, and PDA/TA-ALL@CS are demonstrated in **Figure 6**. For the spectrum of TA, the broad peak at 3300 cm^{-1} is composed of the O-H stretching vibration (Dutta et al., 2021). The 1717 cm^{-1} and 1210 cm^{-1} peaks are accounted for the C=O and C-O stretching vibration, respectively (Dutta et al., 2021; Ricci et al., 2015). The peak at 1618 cm^{-1} belongs to the C=C stretching vibration, and the peak at 760 cm^{-1} is attributed to the O-H in a carboxylic group (Dutta et al., 2021; Ricci et al., 2015). In spectrum c, the broad peak at 3500 cm^{-1} to 3300 cm^{-1} belongs to the N-H and O-H stretching vibration of the ALL@CS nanocapsules, and the peaks located at 2947 cm^{-1}which also appears in the spectrum of ALL@CS (**Figure 1** spectrum a) are assigned to the C-H stretching vibration. These results demonstrated that the ALL@CS existed in this system. Moreover, the absorption peaks contributed by C=O and O-H in the carboxylic group of TA also appeared at 1717 cm^{-1} and 760 cm^{-1}, respectively, on spectrum c, indicating that the TA also existed in this system. Hence, the TA-ALL@CS layer was prepared successfully. For the spectrum of PDA, the broad peak at 3300 cm^{-1} is assigned to the N-H stretching vibration, and the peaks at 1618 cm^{-1} and 1518 cm^{-1} belong to the C=C and C=N stretching vibrations of the benzene ring, respectively (Hao et al., 2019). As for spectrum d, the characterization of the curve is similar with spectrum b from 3500 cm^{-1} to 2500 cm^{-1}, which means the stretching vibration of N-H and O-H from PDA is existing in this coating. Furthermore, the 1516 cm^{-1} peak belongs to the C=N stretching vibration from the benzene ring, revealing that the PDA is introduced in this coating further. The peaks at 1717 cm^{-1} (C=O), 1618 cm^{-1} (C=C), and 760 cm^{-1} (O-H) are witnessed in spectrum d demonstrating that the TA/ALL@CS also appears in such coatings. Hence, the PDA/TA-ALL@CS coatings were prepared by the immersion method successfully.

The thickness of the PDA/TA-ALL@CS-n coating was evaluated using SEM, and the results are shown in **Figures 7A-C**. Interestingly, the thickness of the coatings did not increase when the ratio of the ALL@CS nanocapsules increased. The thickness of the PDA/TA-ALL@CS-6, PDA/TA-ALL@CS-7, and PDA/TA-ALL@CS-8 coatings was ~1.9, ~2.0, and ~1.6 μm, respectively. In the top view of these three coatings, the number of introduced nanocapsules was the most for PDA/TA-ALL@CS-7 coatings (**Figure 7E**). Because the amount of the ALL@CS was fewest in the TA-ALL@CS-8 mixture, there were fewer nanocapsules dispersed in the coatings (**Figure 7F**). While for PDA/TA-ALL@CS-6 coating, with the number of nanocapsules increased, precipitation could occur in the mixture due to electrostatic interaction between TA and the ALL@CS nanocapsules, and restrict the deposition process of the TA-ALL@CS layer.

Antibacterial Properties of PDA/TA-ALL@CS-n Coatings

The colony counting method was used to assess the antibacterial properties of the PDA/TA-ALL@CS-6, PDA/TA-ALL@CS-7, and PDA/TA-ALL@CS-8 coatings. **Figure 8** shows that all these three coatings exhibit good antibacterial effects against *E. coli*, *S. aureus*, and *P. aeruginosa*. In **Figure 8A**, the number of the colonies on the surface of the solid medium is lowest after incubation with PDA/TA-ALL@CS-7 coatings in regard to all these three bacteria, which is about 45, 46, and 46 CFU for *E. coli*, *S. aureus*, and *P. aeruginosa*, respectively. Compared with the control group, the bacteriostasis of these three kinds of bacteria is ~89.2, ~89.2, and ~90.7% (**Figure 8B**), respectively. After

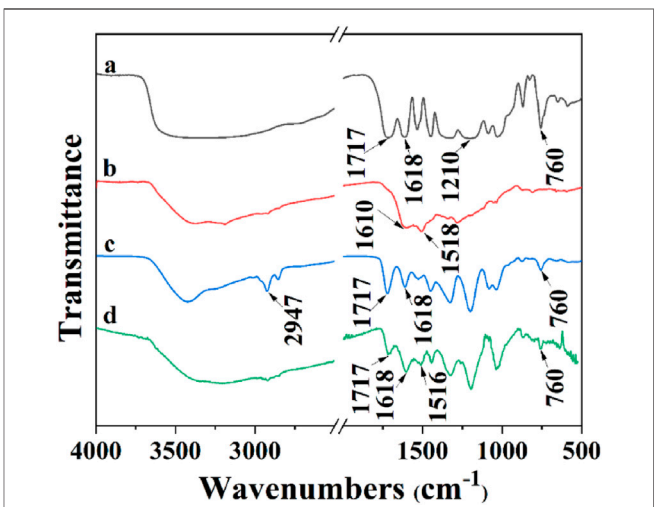

FIGURE 6 | FTIR of TA **(A)**, PDA **(B)**, TA-ALL@CS **(C)**, and PDA/TA-ALL@CS coatings **(D)**.

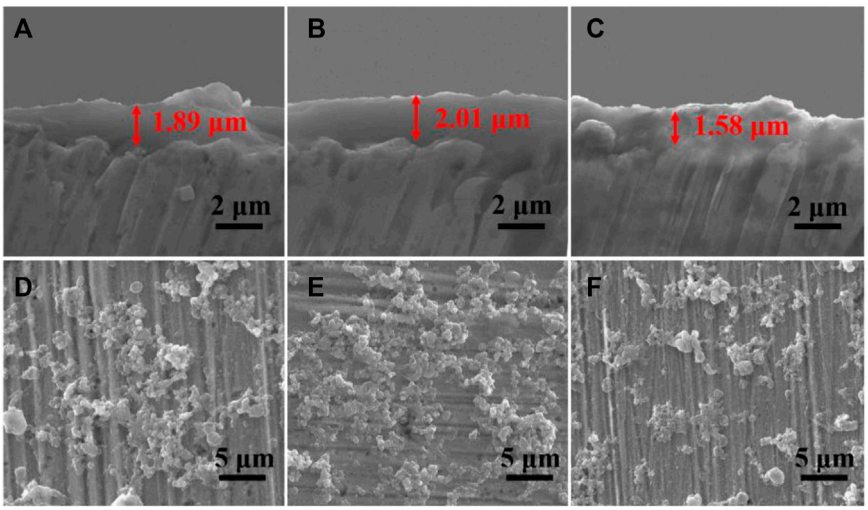

FIGURE 7 | Cross-section and top-view SEM images of PDA/TA-ALL@CS-6 coatings **(A, D)**; PDA/TA-ALL@CS-7 coatings **(B, E)** and PDA/TA-ALL@CS-8 coatings **(C, F)**.

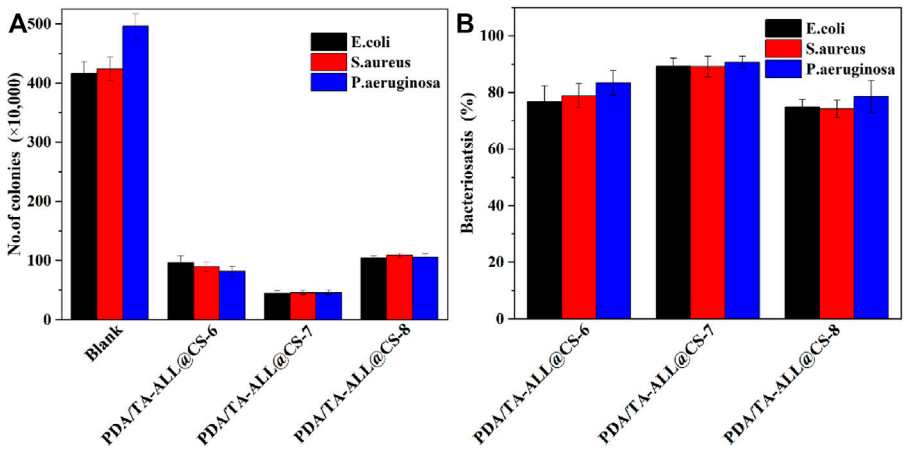

FIGURE 8 | Number of *E. coli*, *S. aureus*, and *P. aeruginosa* bacterial colonies on the solid medium after incubation with the controlled specimen and prepared coatings in Luria-Bertani medium for 18 h **(A)**; the bacteriostasis of *E. coli*, *S. aureus*, and *P. aeruginosa* for the PDA/TA-ALL@CS-n coatings **(B)**. For PDA/TA-ALL@CS-6, PDA/TA-ALL@CS-7, and PDA/TA-ALL@CS-8 coatings, the volume ratios of TA solution to ALL@CS suspension were about 6:4, 7:3, and 8:2, respectively.

incubation with PDA/TA-ALL@CS-8 coated substrates, there are about 104, 109, and 106 CFU on the solid medium, and the antibacterial performance is about 74.9, 74.3, and 78.6% for *E. coli*, *S. aureus*, and *P. aeruginosa*, respectively. According to **Figure 7F**, the number of the introduced ALL@CS nanocapsules is less than that of the other two coatings, which could be the reason why the antibacterial performance is not ideal. Compared with the PDA/TA-ALL@CS-8 group, the antibacterial properties of the PDA/TA-ALL@CS-6 coatings are also lower than the PDA/TA-ALL@CS-7 counterparts, which is decreased by ~12.4, ~10.3, and ~7.3%, respectively.

Generally, the surfaces of the specimens coated with PDA/TA-LL@CS-n have remarkable antibacterial properties. After dying, **Figures 9A–A_2** exhibit almost green spots in view, indicating the bare coupons have little antibacterial properties and nearly all of the bacteria are alive. A few green spots can be witnessed on the PDA/TA-ALL@CS-6 (**Figures 9B–B_2**) and PDA/TA-ALL@CS-8 (**Figures 9D–D_2**), but there are almost all red spots in the view of the PDA/TA-ALL@CS-7 coating surface as seen in a (**Figures 9C–C_2**). This demonstrated that the antibacterial and antifouling effects of the PDA/TA-ALL@CS-7 coating are better than the other coatings. Combined with the results shown in Figures 7D–F, the antibacterial property of the coating was affected by the introduced quantity and dispersion of ALL@CS. Hence, the PDA/TA-ALL@CS-7 coating was selected to evaluate the pH-responsive antibacterial and antifouling bacterial properties.

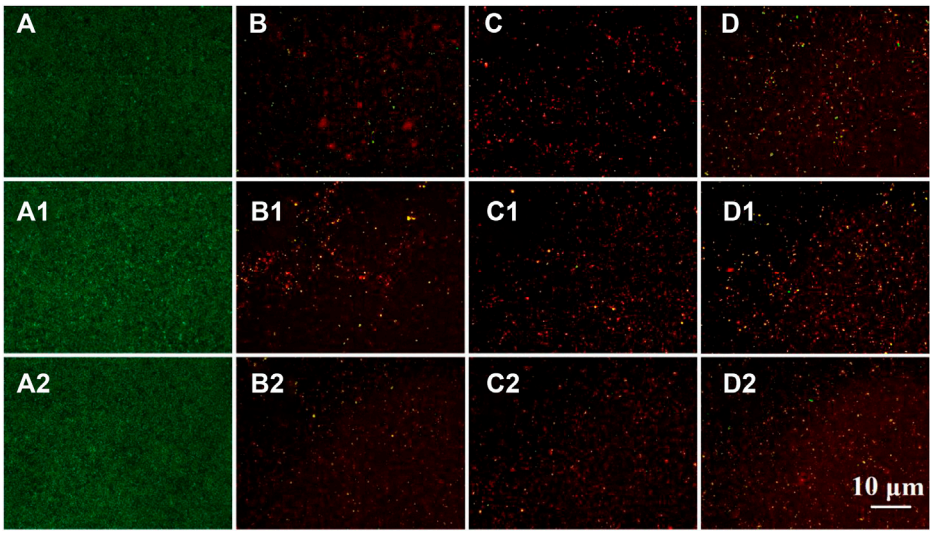

FIGURE 9 | BacLight Live/Dead Kit Assay staining of *E. coli*, *S. aureus*, and *P. aeruginosa* colonized on the bare coupon **(A–A$_2$)**, and the specimens coated with PDA/TA-ALL@CS-6 **(B–B$_2$)**, PDA/TA-ALL@CS-7 **(C–C$_2$)**, PDA/TA-ALL@CS-8 **(D–D$_2$)**, respectively.

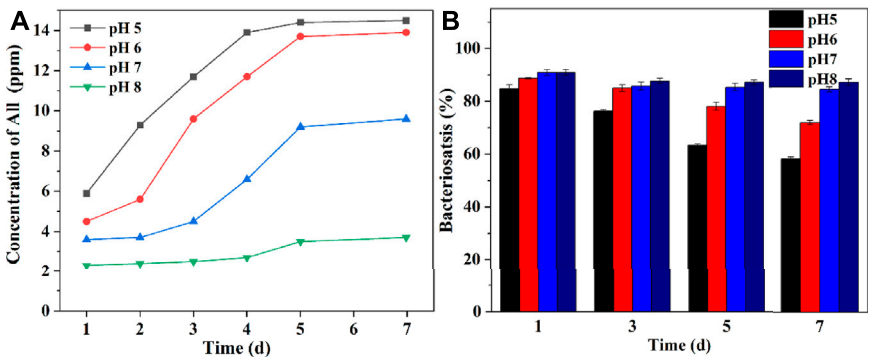

FIGURE 10 | Concentration of ALL released from the PDA/TA-ALL@CS-7 coatings in different pH PBS solutions **(A)**. The bacteriostasis of the PDA/TA-ALL@CS-7 coatings against *P. aeruginosa* after being immersed in different pH PBS solutions for seven days **(B)**.

pH-Responsive Properties of the PDA/TA-ALL@CS Coatings

The releasing behaviors of ALL and the antibacterial properties of the immersed PDA/TA-ALL@CS coatings in different pH PBS (pH 5, 6, 7, and 8) were evaluated using UV-Vis and the colony counting method. In **Figure 10A**, with the increasing pH value of the PBS, the concentration of the released ALL from the coating decreases apparently. After seven days of immersion in pH 5, the amount of released ALL increased gradually from~5.9 ppm to ~14.5 ppm. The concentration of released ALL increased from ~4.5 to ~13.9 ppm after immersion in pH 6 solutions. The release of the ALL was more rapid in the first five days. When the coated coupon was immersed in a neutral solution, the release of the ALL became slower, which was about 3.6, 4.5, 9.2, and 9.6 ppm for released ALL from one, three, five, and seven days, respectively. Because the protonation of the nanocapsules was restricted in an alkaline environment, the amount of the released ALL was maintained at a very low level (3.7 ppm) after immersion in pH 8 PBS solutions for seven days. Hence, the PDA/TA-ALL@CS coatings showed good pH-responsive properties and could restrict the release of antifoulants in the marine environment when bacterial reproduction did not occur.

To further determine the antibacterial effects of PDA/TA-ALL@CS coatings, the bacteriostasis of the PDA/TA-ALL@CS coatings against *P. aeruginosa* after immersion in different pH solutions for seven days is shown in **Figure 10B**. The antibacterial efficiency decreased dramatically after immersion in an acidic environment but was maintained at a high level after immersion in an alkaline environment. The antibacterial properties decreased from ~84.7% after one day to ~58.1% after seven days of immersion in pH 4 PBS solution. As for the pH 5 group, the bacteriostasis rate decreased from ~88.7% after one day to 71.9% after seven days. However, after immersion

in a neutral PBS for seven days, the bacteriostasis only decreased by ~6.4%. When immersed in an environment with a pH value similar to seawater (pH 8), the PDA/TA-ALL@CS coating could maintain an outstanding antibacterial property after seven days, which was ~87.1% (decreased by 3.7%). The above results demonstrated that the PDA/TA-ALL@CS coatings maintained remarkable antibacterial and antifouling properties after immersion for seven days in an alkaline environment, and released ALL to kill bacteria when the pH of the microenvironment was decreased by bacterial reproduction.

CONCLUSION

In this work, the ALL@CS nanocapsules are synthesis by the emulsion method. These nanocapsules exhibit outstanding antibacterial properties against *E. coli*, *S. aureus*, and *P. aeruginosa*. Because of the protonation of CS, the ALL@CS nanocapsules have pH-responsive properties, which can release an amount of ALL in acidic environments and maintain the releasing rate at a low level in alkaline environments. When preparation of the PDA/TA-ALL@CS coatings, the volume ratio of TA and nanocapsules affects the amount of ALL@CS introduced on the coating, and the proper parameters are 7:3 of the volume ratio. The antibacterial and antifouling properties of PDA/TA-ALL@CS-7 coatings are best against *E. coli*, *S. aureus*, and *P. aeruginosa*, and the bacteriostasis is all above 89.2%. Moreover, the PDA/TA-ALL@CS-7 coatings also process pH-responsive properties. The releasing behaviors of ALL differ greatly under seven days of immersion in different pH environments. The ALL release was faster in an acidic environment and slower in an alkaline environment. The ALL contained in the PDA/TA-ALL@CS coating impacts the antibacterial performance directly. After seven days of immersion in pH 8 environment solution, the bacteriostasis of the coatings was still about 87.2%. This work of PDA/TA-ALL@CS coatings supports the idea to design smart antifouling coatings and solve the biofouling problems at the anchoring state.

DATA AVAILABILITY STATEMENT

The original contributions presented in the study are included in the article/Supplementary Material, further inquiries can be directed to the corresponding authors.

AUTHOR CONTRIBUTIONS

XH: investigation, methodology, and writing—original draft. WY: investigation and methodology. ZS: investigation and methodology. JY: investigation. YB: investigation. HQ: investigation. TC: investigation, supervision, and writing-review and editing. DZ: supervision, conceptualization, methodology, writing—original draft, and writing—review and editing. All the authors contributed to the discussion of the work.

FUNDING

The work was supported by the China Postdoctoral Science Foundation (2021M700381) and the Postdoctoral Research Foundation of Shunde Graduate School of University of Science and Technology Beijing (2021BH003).

REFERENCES

Ankri, S., and Mirelman, D. (1999). Antimicrobial Properties of Allicin from Garlic. *Microbes Infect.* 1, 125–129. doi:10.1016/s1286-4579(99)80003-3

Arifin, D. Y., Lee, L. Y., and Wang, C.-H. (2006). Mathematical Modeling and Simulation of Drug Release from Microspheres: Implications to Drug Delivery Systems. *Adv. Drug Deliver. Rev.* 58, 1274–1325. doi:10.1016/j.addr.2006.09.007

Bagley, F., Atlar, M., Charles, A., and Anderson, C. (2015). The Use of Copper-Based Antifoulings on Aluminium Ship Hulls. *Ocean Eng.* 109, 595–602. doi:10.1016/j.oceaneng.2015.09.044

Banerjee, I., Pangule, R. C., and Kane, R. (2011). Antifouling Coatings: Recent Developments in the Design of Surfaces that Prevent Fouling by Proteins, Bacteria, and marine Organisms. *Adv. Mater.* 23, 690–718. doi:10.1002/adma.201001215

Bhatwalkar, S. B., Mondal, R., Krishna, S. B. N., Adam, J. K., Govender, P., and Anupam, R. (2021). Antibacterial Properties of Organosulfur Compounds of Garlic (Allium Sativum). *Front. Microbiol.* 12, 613077. doi:10.3389/fmicb.2021.613077

Bloecher, N., Solvang, T., and Floerl, O. (2021). Efficacy Testing of Novel Antifouling Systems for marine Sensors. *Ocean Eng.* 240, 109983. doi:10.1016/j.oceaneng.2021.109983

Breyer, K. (2013). Evaluating the Efficacy of a Low-Dose Garlic Compound (Allicin) against Infection with Aeromonas Salmonicida in Rainbow trout. *Acta Microbiol. Imm. H.* http://hdl.handle.net/1813/34286.

Cao, H., Zhu, K., Fan, J., and Qiao, L. (2014). Garlic-derived Allyl Sulfides in Cancer Therapy. *Anticancer Agents Med. Chem.* 14, 793–799. doi:10.2174/1871520614666140521120811

Chen, H., Zhi, H., Liang, J., Yu, M., Cui, B., Zhao, X., et al. (2021). Development of Leaf-Adhesive Pesticide Nanocapsules with pH-Responsive Release to Enhance Retention Time on Crop Leaves and Improve Utilization Efficiency. *J. Mater. Chem. B.* 9, 783–792. doi:10.1039/d0tb02430a

Dutta, N., Hazarika, S., and Maji, T. K. (2021). Study on the Role of Tannic Acid–Calcium Oxide Adduct as a green Heat Stabilizer as Well as Reinforcing Filler in the Bio-Based Hybrid Polyvinyl Chloride–Thermoplastic Starch Polymer Composite. *Polym. Eng. Sci.* 61, 2339–2348. doi:10.1002/pen.25761

Greef, D., Barton, E. M., Sandberg, E. N., Croley, C. R., Pumarol, J., Wong, T. L., et al. (2021). Anticancer Potential of Garlic and its Bioactive Constituents: A Systematic and Comprehensive Review. *Semin. Cancer Biol.* 73, 219–264. doi:10.1016/j.semcancer.2020.11.020

Gu, H., Xu, X., Zhang, H., Liang, C., Lou, H., Ma, C., et al. (2018). Chitosan-coated-magnetite with Covalently Grafted Polystyrene Based Carbon Nanocomposites for Hexavalent Chromium Adsorption. *Eng. Sci.* 1, 46–54. doi:10.30919/es.180308

Hao, X., Chen, S., Qin, D., Zhang, M., Li, W., Fan, J., et al. (2020). Antifouling and Antibacterial Behaviors of Capsaicin-Based pH Responsive Smart Coatings in marine Environments. *Mater. Sci. Eng. C Mater. Biol. Appl.* 108, 110361. doi:10.1016/j.msec.2019.110361

Hao, X., Chen, S., Yu, H., Liu, D., and Sun, W. (2016). Metal Ion-Coordinated Carboxymethylated Chitosan Grafted Carbon Nanotubes with Enhanced Antibacterial Properties. *RSC Adv.* 6, 39–43. doi:10.1039/c5ra21003h

Hao, X., Wang, W., Yang, Z., Yue, L., Sun, H., Wang, H., et al. (2019). pH Responsive Antifouling and Antibacterial Multilayer Films with Self-Healing Performance. *Chem. Eng. J.* 356, 130–141. doi:10.1016/j.cej.2018.08.181

Hathout, R. M., Metwally, A. A., El-Ahmady, S. H., Metwally, E. S., Ghonim, N. A., Bayoumy, S. A., et al. (2018). Dual Stimuli-Responsive Polypyrrole

Nanoparticles for Anticancer Therapy. *J. Drug Deliv. Sci. Tec.* 47, 176–180. doi:10.1016/j.jddst.2018.07.002

Hosseini, S. F., Ghaderi, J., and Gómez-Guillén, M. C. (2022). Tailoring Physico-Mechanical and Antimicrobial/antioxidant Properties of Biopolymeric Films by Cinnamaldehyde-Loaded Chitosan Nanoparticles and Their Application in Packaging of Fresh Rainbow trout Fillets. *Food Hydrocolloid.* 124, 107249. doi:10.1016/j.foodhyd.2021.107249

Huang, L., Lou, Y., Zhang, D., Ma, L., and Li, X. (2019). d -Cysteine Functionalised Silver Nanoparticles Surface with a "Disperse-Then-Kill" Antibacterial Synergy. *Chem. Eng. J.* 381, 122662. doi:10.1016/j.cej.2019.122662

Huang, X., Mutlu, H., and Theato, P. (2020). A Bioinspired Hierarchical Underwater Superoleophobic Surface with Reversible pH Response. *Adv. Mater. Inter.* 7, 2000101. doi:10.1002/admi.202000101

Janik-Hazuka, M., Kamiński, K., Kaczor-Kamińska, M., Szafraniec-Szczęsny, J., Kmak, A., Kassassir, H., et al. (2021). Hyaluronic Acid-Based Nanocapsules as Efficient Delivery Systems of Garlic Oil Active Components with Anticancer Activity. *Nanomaterials.* 11, 1354. doi:10.3390/nano11051354

Janská, P., Knejzlík, Z., Perumal, A. S., Jurok, R., Tokárová, V., Nicolau, D. V., et al. (2021). Effect of Physicochemical Parameters on the Stability and Activity of Garlic Alliinase and its Use for *In-Situ* Allicin Synthesis. *Plos One.* 16, e0248878. doi:10.1371/journal.pone.0248878

Jia, Z., Liu, Y., Wang, Y., Gong, Y., Jin, P., Suo, X., et al. (2017). Technology, Flame spray Fabrication of Polyethylene-Cu Composite Coatings with Enwrapped Structures: A New Route for Constructing Antifouling Layers. *Surf. Coat. Tech.* 309, 872–879. doi:10.1016/j.surfcoat.2016.10.071

Kumar, H., Yadav, V., Saha, S. K., and Kang, N. (2021). Adsorption and Inhibition Mechanism of Efficient and Environment Friendly Corrosion Inhibitor for Mild Steel: Experimental and Theoretical Study. *J. Mol. Liq.* 338, 116634. doi:10.1016/j.molliq.2021.116634

Lawrie, G., Keen, I., Drew, B., Chandler-Temple, A., Rintoul, L., Fredericks, P., et al. (2007). Interactions between Alginate and Chitosan Biopolymers Characterized Using FTIR and XPS. *Biomacromolecules.* 8, 2533–2541. doi:10.1021/bm070014y

Lawson, L. D., and Hughes, B. G. (1992). Characterization of the Formation of Allicin and Other Thiosulfinates from Garlic, Planta. *Med.* 58, 345–350. doi:10.1055/s-2006-961482

Lee, K. Y., and Mooney, D. J. (2012). Alginate: Properties and Biomedical Applications. *Prog. Polym. Sci.* 37, 106–126. doi:10.1016/j.progpolymsci.2011.06.003

Lejars, M., Margaillan, A., and Bressy, C. (2012). Fouling Release Coatings: A Nontoxic Alternative to Biocidal Antifouling Coatings. *Chem. Rev.* 112, 4347–4390. doi:10.1021/cr200350v

Lin, C.-C., and Metters, A. T. (2006). Hydrogels in Controlled Release Formulations: Network Design and Mathematical Modeling. *Adv. Drug Deliver. Rev.* 58, 1379–1408. doi:10.1016/j.addr.2006.09.004

Liu, M., Li, S., Wang, H., Jiang, R., and Zhou, X. (2021). Research Progress of Environmentally Friendly marine Antifouling Coatings. *Polym. Chem.* 12, 3702–3720. doi:10.1039/d1py00512j

Qian, H., Yang, J., Lou, Y., and Rahman, O. (2019). Mussel-inspired Superhydrophilic Surface with Enhanced Antimicrobial Properties under Immersed and Atmospheric Conditions. *Appl. Surf. Sci.* 465, 267–278. doi:10.1016/j.apsusc.2018.09.173

Qian, H., Liu, S., Wang, P., Huang, Y., Lou, Y., Huang, L., et al. (2007a). Investigation of Microbiologically Influenced Corrosion of 304 Stainless Steel by Aerobic Thermoacidophilic Archaeon Metallosphaera Cuprina. *Bioelectrochemistry.* 136, 107635.

Qian, P. Y., Lau, S. C. K., Dahms, H. U., Dobretsov, S., and Harder, T. (2007b). Marine Biofilms as Mediators of Colonization by marine Macroorganisms: Implications for Antifouling and Aquaculture. *Mar. Biotechnol.* 9, 399–410. doi:10.1007/s10126-007-9001-9

Ricci, A., Olejar, K. J., Parpinello, G. P., Kilmartin, P. A., and Versari, A. (2015). Application of Fourier Transform Infrared (FTIR) Spectroscopy in the Characterization of Tannins. *Appl. Spectrosc. Rev.* 50, 407–442. doi:10.1080/05704928.2014.1000461

Saadouli, I., Mosbah, A., Ferjani, R., Stathopoulou, P., Galiatsatos, I., Asimakis, E., et al. (2021). The Impact of the Inoculation of Phosphate-Solubilizing Bacteria Pantoea Agglomerans on Phosphorus Availability and Bacterial Community Dynamics of a Semi-arid Soil. *Microoganisms.* 9, 1661. doi:10.3390/microorganisms9081661

Tian, B., Cheng, J., Zhang, T., Liu, Y., and Chen, D. (2022). Multifunctional Chitosan-Based Film Loaded with Hops β-acids: Preparation, Characterization, Controlled Release and Antibacterial Mechanism. *Food Hydrocolloid.* 124, 107337. doi:10.1016/j.foodhyd.2021.107337

Traba, C., and Liang, J. F. (2015). Bacteria Responsive Antibacterial Surfaces for Indwelling Device Infections. *J. Control Release.* 198, 18–25. doi:10.1016/j.jconrel.2014.11.025

Wang, W., Hao, X., Chen, S., Yang, Z., and Guo, Z. (2018). pH-Responsive Capsaicin@chitosan Nanocapsules for Antibiofouling in marine Applications. *Polymer.* 158, 223–230. doi:10.1016/j.polymer.2018.10.067

Wills, E. D. (1956). Enzyme Inhibition by Allicin, the Active Principle of Garlic. *Biochem. J.* 63, 514–520. doi:10.1042/bj0630514

Xu, G., Neoh, K. G., Kang, E.-T., and Teo, S. L.-M. (2020). Switchable Antimicrobial and Antifouling Coatings from Tannic Acid-Scaffolded Binary Polymer Brushes. *ACS Sustain. Chem. Eng.* 8, 2586–2595. doi:10.1021/acssuschemeng.9b07836

Yan, T., He, J., Liu, R., Liu, Z., and Cheng, J. (2020). Chitosan Capped pH-Responsive Hollow Mesoporous Silica Nanoparticles for Targeted Chemo-Photo Combination Therapy. *Carbohyd. Polym.* 231, 115706. doi:10.1016/j.carbpol.2019.115706

Yang, J., Qian, H., Wang, J., Ju, P., Lou, Y., Li, G., et al. (2021). Mechanically Durable Antibacterial Nanocoatings Based on Zwitterionic Copolymers Containing Dopamine Segments. *J. Mater. Sci. Technol.* 89, 233–241. doi:10.1016/j.jmst.2020.11.031

Yebra, D. M., Kiil, S., and Dam-Johansen, K. (2004). Antifouling Technology-Past, Present and Future Steps towards Efficient and Environmentally Friendly Antifouling Coatings. *Prog. Org. Coat.* 50, 75–104. doi:10.1016/j.porgcoat.2003.06.001

Yunessnia lehi, A., Shagholani, H., Ghorbani, M., Nikpay, A., Soleimani lashkenari, M., and Soltani, M. (2019). Chitosan Nanocapsule-Mounted Cellulose Nanofibrils as Nanoships for Smart Drug Delivery Systems and Treatment of Avian Trichomoniasis. *J. Taiwan Inst. Chem. E* 95, 290–299. doi:10.1016/j.jtice.2018.07.014

Zhang, Y., Liu, X., Ruan, J., Zhuang, X., Zhang, X., and Li, Z. (2020). Pharmacotherapy, Phytochemicals of Garlic: Promising Candidates for Cancer Therapy. *Biomed. Pharmacother.* 123, 109730. doi:10.1016/j.biopha.2019.109730

Zhou, Y., Feng, J., Peng, H., Guo, T., Xiao, J., Zhu, W., et al. (2021). Allicin Inclusions with α-cyclodextrin Effectively Masking its Odor: Preparation, Characterization, and Olfactory and Gustatory Evaluation. *J. Food Sci.* 86, 4026–4036. doi:10.1111/1750-3841.15882

Conflict of Interest: The authors declare that the research was conducted in the absence of any commercial or financial relationships that could be construed as a potential conflict of interest.

Publisher's Note: All claims expressed in this article are solely those of the authors and do not necessarily represent those of their affiliated organizations, or those of the publisher, the editors, and the reviewers. Any product that may be evaluated in this article, or claim that may be made by its manufacturer, is not guaranteed or endorsed by the publisher.